Interaction between heterogeneous and homogeneous reaction of premixed hydrogen-air mixture in a planar catalytic micro-combustor

Qingbo Lu [a], Jianfeng Pan [a *], Wenming Yang [b], Aikun Tang [a], Stephen Bani [a], Xia Shao [a]

[a] School of Energy and Power Engineering, Jiangsu University, Zhenjiang 212013, China

[b] Department of Mechanical Engineering, National University of Singapore, 117576, Singapore

*Corresponding author: Dr. Jianfeng Pan

Address: School of Energy and Power Engineering, Jiangsu University, Zhenjiang 212013, China

Tel.: +86-0511-88780210

Fax: +86-0511-88780216

E-mail address: mike@ujs.edu.cn

ABSTRACT

Hetero-/homogeneous combustion of hydrogen-air mixture in a platinum-coated micro channel was studied by means of three-dimensional (3D) Computational Fluid Dynamics (CFD) model using detailed reaction mechanisms for homogeneous (gas phase) and heterogeneous (catalytic) reactions. The influence of heterogeneous reaction on homogeneous reaction was obtained by discussing the hetero-/homogeneous reaction characteristics, the process and competitiveness of heterogeneous reaction. Intense depletion of fuel and product formation near the inlet has shown that fuel absorption reaction was predominant whiles there was no homogeneous reaction. The free radicals from homogeneous reaction near the catalytic surface were drained, resulting in the interruption of chain reaction. The desorbed product as the third-body promoted the chain terminating reaction to deactivate free radical. The competitiveness value of heterogeneous reaction for capturing fuel was 14.85%, indicating a weak reaction intensity in the catalytic combustor. The heterogeneous reaction presented an inhibition effect on homogeneous reaction but greatly enhanced the combustion efficiency in the micro channel.

Keywords: Micro combustion, Hydrogen, Heterogeneous and homogeneous reaction, Catalysis, Numerical simulation

1. Introduction

Micro combustors have received much attention in the combustion research community recently, due to their conspicuous advantages. These include high energy density, low processing cost and being environmental friendly [1, 2]. The micro reactors are used as heat source in micro power devices and also acted as micro-reformers to create hydrogen for fuel cells [3-7]. It has been established that, with decreasing size of the combustor, there are more unforeseen factors that influence the combustion process in the channel. For example, the occurrence of unstable flame ascribed to a high surface-to-volume ratio, increasing heat loss to the surrounding, and thermal and radical quenching on the wall. Therefore, many useful strategies have been proposed to settle these issues and extend the operating range of micro scale combustion. These are applying heat-recirculating combustors to reduce heat losses [8, 9], the utilization of quenching resistant fuel [10-12] and employing catalytic combustors to enhance reaction rate and suppress radical depletion [13-15]. In the case of heterogeneous catalysis, high surface-to-volume ratio is beneficial to initiate catalytic reaction in micro combustors and it is considered as one of the best available methods to conquer these defects encountered in the miniaturization process. The catalysis can inhibit the intrinsic flame, extend the classical flammability limits and enhance the combustion stability even in the condition of excessive heat losses [16, 17].

In the catalytic channel, different physical and chemical processes are intertwined, leading to the difficulty in understanding the interaction between heterogeneous and homogeneous reactions. It has been demonstrated that the exothermicity of catalytic reaction could facilitate flame combustion, and a competition for reactants between catalytic and conventional combustion could suppress the homogeneous reaction. The catalytically coated walls in the micro- and meso-scale channels mitigated

the intrinsic flame instabilities, and the suppression of the flame dynamics could be attributed to the theoretically predicted diminishing sensitivity of the homogeneous ignition distance to small perturbations of the gaseous reactivity with increasing catalytic reactivity [18, 19]. The homogeneous ignition distance was due mainly to the gaseous pathway, and the catalytic pathway affected homogeneous ignition indirectly via the transport of the deficient reactant (fuel) [20]. Compared to the non-catalytic combustor, the catalytic combustor displayed a weak gas-phase reaction intensity [21]. In addition, the homogeneous ignition temperature increased in the presence of platinum as compared to inert surfaces, this was suppressed by catalytic formation of H_2O and the adsorption of hydrogen atom, and could be impacted by multi-component transport phenomena [22, 23]. For the competition between surface and gas chemistries at the vicinity of the catalytic surface, Deutschmann et al. [24] demonstrated that two competitions (fuel and oxidizer) were driven by sticking probability of species on the surface. Nevertheless, the catalytic reaction can significantly enhance the combustion efficiency in a catalytic micro-combustor according to Haruta et al. [25].

In the catalytic combustor, the lean limitations of gas-phase reactions were negligible when compared to the surface reactions [26]. The characteristic dimension of the channel was less than the quenching distance of fuel, thus the gas-phase reaction was neglected in the chemistry schemes [11]. The gas-phase reactions should be taken into account in the catalytic combustor when the characteristic dimension of the channel is in critical quenching distance of fuel. Appel et al. [26] experimentally and numerically analyzed the gas-phase ignition of fuel-lean hydrogen/air mixtures over platinum (Pt) in the single channel. Their results indicated that the discrepancies between measured and predicted gas-phase ignition distances were mainly due to the gas-phase reaction pathway. For the interplay between the gas-phase and catalytic reactions, Chen et al. [27] depicted the overall picture of gas-phase

and catalytic reaction interaction under inlet velocity versus a function of channel diameter. The main reaction was dominant in the different regions separately. Moreover, Ghermay et al. [28] investigated the effect of practical channels with different geometrical confinements on evaluating the significance of gas-phase chemistry at different pressures, temperatures and mass throughputs. Finally, the comprehensive effect of desorbed species from the catalytic reaction inhibited the gas-phase reactions, because a small amount of desorbed species had the promotional effect on gas-phase reactions [29].

In the hetero-/homogeneous reactions, the relationship between the homogeneous and heterogeneous reactions is yet not clearly illustrated and needs further research, especially for the premixed H_2/air under an equivalence ratio of 1.0 at a low flow velocity. In our previous work [29, 30], it was shown that the homogeneous reaction could be suppressed by the heterogeneous reaction observed from the hetero-/homogeneous reaction characteristics for H_2/O_2 mixture in the catalytic combustor. The interaction between heterogeneous reaction and homogeneous reaction was effected by catalyst segment layout and size of catalytic wall. In this work, we study the combustion of premixed H_2/air mixture in the micro channel coated with platinum by numerical simulation. The hetero-/homogeneous reaction characteristics, the process and competitiveness of heterogeneous reaction after the homogeneous ignition in the catalytic combustor are investigated to obtain the influence of heterogeneous reaction on homogeneous reaction.

2. Physical and Mathematical models

2.1. Physical Model

A conventional micro combustor with a rectangular channel was employed in this work, as shown in Fig. 1. The dimensions are 1 mm in length (- *x*, L), 10 mm in width (- *y*, W), 1 mm in height (- *z*, H) and the wall thickness (Ws) is 0.5 mm. The inner surface of the combustor was coated with platinum

catalyst with a surface site density of 2.7×10^{-9} mol/cm^2. The wall material of the combustor was made of 316L stainless steel due to its high thermostability [3]. For the operation process, the premixed hydrogen/air mixture flowed through the straight channel. A rectangular inlet was set at the left of the combustor, and an outlet was set at the other end of the combustor.

A structured grid was adopted in the computational domain, and Fluent software was employed for the simulation [31]. Due to the symmetrical structure of the combustor, half of its space was used for the computational domain to save calculation time. Centerline gaseous temperature profiles in the channel were compared for different grid sizes, as shown in Fig. 2. The mesh near the wall was locally refined and 165000 cells (100×110×15 cells used in each X-Y-Z direction) were used in the computational domain. In this regards, the optimized grid can save computational time and meet the precision requirement.

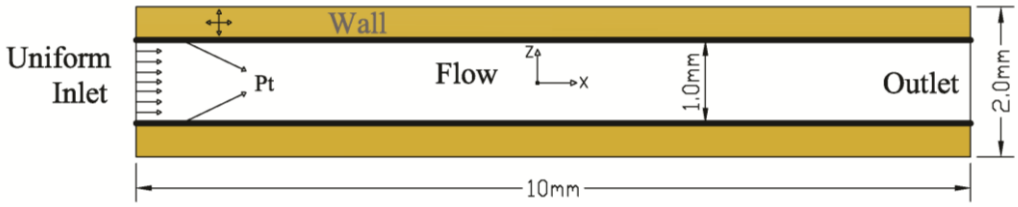

Fig. 1. Schematic of the combustor model.

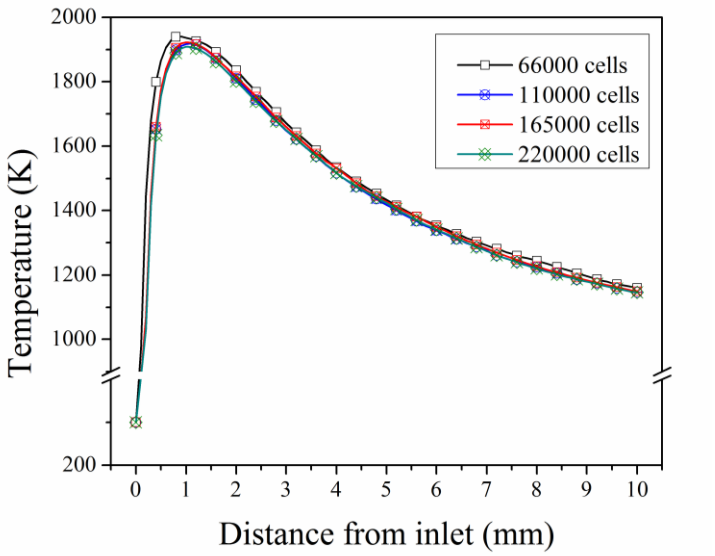

Fig. 2. Distribution of the centerline temperature in the combustor with different mesh densities.

2.2. Methods of model building

In this simulation, the Knudsen number was less than the critical value of 0.001, thus the continuous flow was considered for the mixture. The laminar model was adopted due to the low Reynolds number (Reynolds number of 149 in this study). Governing equations of continuity, momentum, species and energy were discretized by the second order upwind schemes in the numerical model. The detailed methods for calculating the mixture properties were chosen from our previous study [30]. The SIMPLE algorithm was proposed to manage the pressure-velocity coupling. The simulation was deemed to have converged when the residuals of all governing equations were smaller than 10^{-6}.

A reaction mechanism proposed by Li et al. [32] was used for gas phase reaction, which comprised 9 species and 21 reversible reactions. The surface chemistry mechanism of Deutschmann et al. [33] was employed to describe the oxidation of hydrogen over platinum. Five surface species: Pt(s), H(s), H_2O(s), OH(s) and O(s) described the coverage of absorbed species on the catalytic surface. Pt(s) as free surface site was beneficial to adsorption. The detailed reaction mechanisms were employed in previous studies [14, 26] and a good agreement between simulation and experimental data were indicated. The transport database of CHEMKIN was used for mixture diffusion properties [34]. Surface and gas-phase chemical reaction rates were estimated with CHEMKIN [35] and Surface CHEMKIN [36], respectively.

The boundary conditions of the inlet and outlet were set as velocity-inlet and outflow, respectively. The hydrogen-air equivalence ratio was 1.0. In this work, the initial temperatures of the inlet mixture and combustor wall are both specified at 300 K, and the atmospheric pressure was set as 101 KPa. A

non-slip condition was used as the boundary condition on the wall. The heat loss from the outer wall to the surrounding air was given by Eq. (1).

$$q'' = h(Tw-300) + \varepsilon\sigma\,(Tw^4-300^4) \quad (1)$$

where Tw is outer surface temperature, h is natural convection coefficient (20 $W/m^2/K$), σ is Stephan-Boltzmann constant (5.67×10^{-8} $W/m^2/K^4$) and ε is the solid surface emissivity (0.65) in this work.

2.3. Validation of the Model

The set-up of the experiment could be found in the work of Tang et al. [37]. The experimental and simulation data were compared under the same conditions, which were an inlet velocity of 1.5 m/s and an equivalence ratio of 1.0. Fig. 3 shows the centerline temperature profiles on the external surface of non-/catalytic wall for both the experiment and simulation. The maximum deviations between the simulation and experimental results were 1.8% (with a non-catalytic wall) and 3.1% (with a catalytic wall). A minor deviation shows a good agreement, demonstrating a rational accuracy of the numerical model employed in this work.

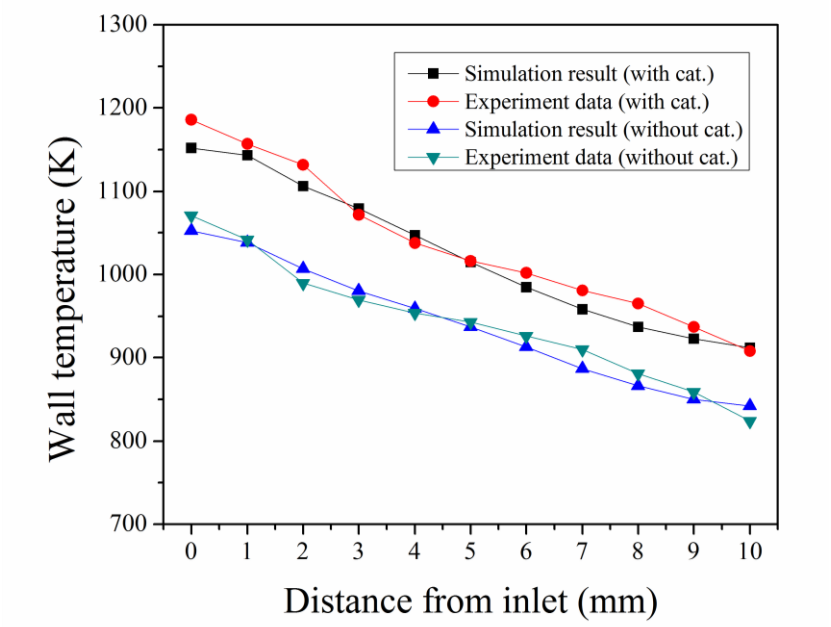

Fig. 3. Centerline temperature distributions on the outer surface from experiment and simulation under different conditions.

3 Results and discussion

3.1. Combustion characteristics of hetero-/homogeneous reaction

In the catalytic combustor, the combustion characteristics for H_2-air mixture and the influence of heterogeneous reaction on homogeneous reaction are systematically investigated by numerical simulation. The initial conditions of reactants in the inlet are listed below; the equivalence ratio of 1.0, the initial temperature of 300 K and flow velocity of 1.5 m/s. For the reference case, the non-catalytic combustor was employed to obtain purely homogeneous reaction under the same boundary conditions. The heterogeneous and homogeneous reaction model in catalytic combustor is denoted as HH, whiles the purely homogeneous reaction model is denoted as HR.

Fig. 4 shows the computed contour of temperature distribution in X-Y plane for HH and HR. It can be seen from Fig. 4 that, the high temperature region in the channel has a trapezoid shape, and the size of the region in HH is larger than that in HR. The temperature distributions on the centerline of the channel are displayed in Fig. 5, to show clearly the temperature distribution in the channel. The temperature on the centerline of the channel first increases and then decreases slowly, and the peak temperature of HR in the channel is 87 K higher than that of HH. The decreased flame temperature indicates that the homogeneous reaction is inhibited in the catalytic combustor due to the existence of the heterogeneous reaction. It is a fact that the OH concentration distributions generally describe the reaction zone and high temperature zone in the homogenous combustion [15, 38]. The OH concentration distribution on the centerline of the channel is shown in Fig. 5. The OH concentration on the centerline of the channel first increases and then decreases sharply. The maximum OH mass

fraction of HR in the channel is 6.5 E-05 higher than that of HH, suggesting an inhibition effect of heterogeneous reaction on homogeneous reaction during the catalytic combustion process. Furthermore, the decreased trend of OH concentration in HH is more pronounced as compared to that of HR. It indicates the existence of inhibition effect in the channel.

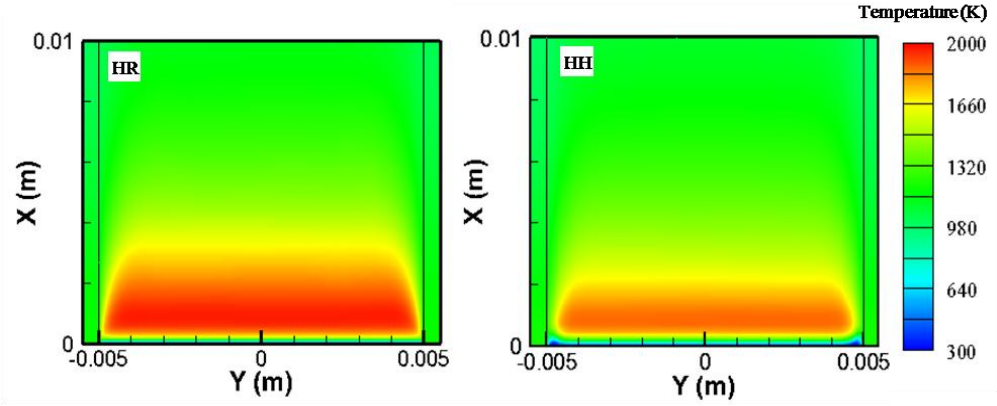

Fig. 4 Computed contour of temperature distribution in X-Y plane for HH and HR.

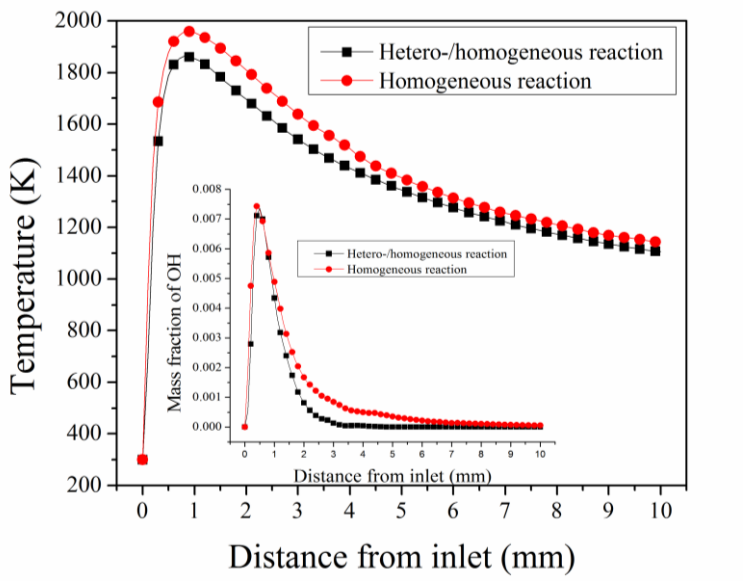

Fig. 5. Temperature and OH concentration distribution on the centerline of the channel.

Fig. 6 shows the averaged mass fractions of major species over the Y-Z plane from inlet to outlet. The intermediate mass fraction (i.e. H atom) is decreasing in HH as compared with HR, suggesting the inhibition effect of heterogeneous reaction on homogeneous reaction. The decreased intermediate is caused by the absorption and the fuel competition between heterogeneous and homogeneous reaction

and it accounts for the decreasing homogeneous reaction intensity. Furthermore, it is noted that the fuel consumption and the created H_2O in the HH are more than that in HR. As expected, the H_2 conversion rate in HH (up to 98.7%) is 8% higher than that of HR. Hence, the combustion efficiency of catalytic combustor is enhanced significantly when compared with that of the conventional combustor.

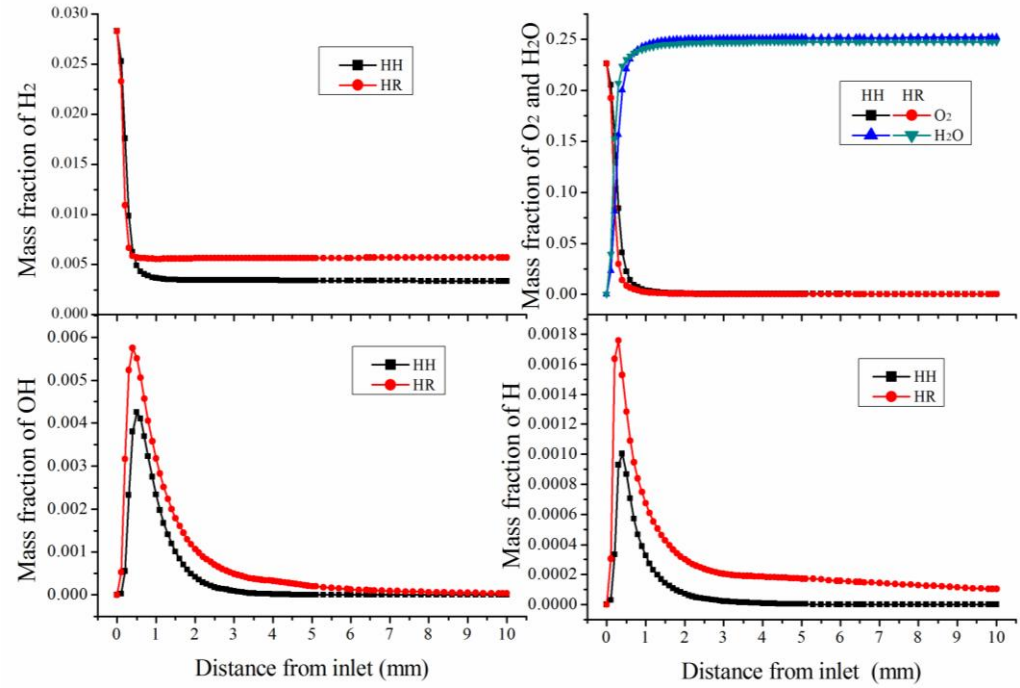

Fig. 6. Major species mass fractions averaged over the Y-Z plane.

3.2. Process of heterogeneous reaction

The absorption reaction of gaseous species plays an important role in the reactants competition between the heterogeneous reaction and homogeneous reaction. The competed reactants are used to initiate the heterogeneous reaction at a low temperature due to the absorption ability of Pt catalyst. In other words, the absorption reaction first occurs and consumes part of the fresh reactants in the heterogeneous reaction.

The net destruction reaction rate of gaseous species on the catalytic surface is shown in Fig. 7. The net destruction reaction rate of gaseous species is the difference between absorption reaction rate and desorption reaction rate of the same species. The reaction rate of positive denotes the consumption of

gaseous species, while the reaction rate of negative denotes the creation of gaseous species. The destruction rates of OH radical and oxygen atom are multiplied by a given factor of 100 to distinguish between the different rates. When a destruction reaction with high reaction rate occurs at a zone, it means that this reaction is a dominant reaction at this zone. Thus, there are three stages of the heterogeneous reaction on the catalytic surface; the rapid depletion of reactants near the inlet (region I), fast consumption of free radicals (region II) and reaction balance state in the downstream (region III). The region I is about 0.3 mm of length from the inlet, and the reactants absorption reactions and product desorption reaction are dominant in the zone, due to the adequate incoming mixture in the inlet. The temperature of incoming mixture (300 K) is much lower than the ignition temperature of H_2, even though H_2 is highly flammable. In this case, the homogeneous reaction is not immediately ignited at the inlet, but the catalytic reaction of H_2 is initiated at room temperature. The incoming mixture is fast depleted near the catalytic surface and the destruction reaction rates of reactants are highest at inlet. The heterogeneous reaction plays a dominant role in region I.

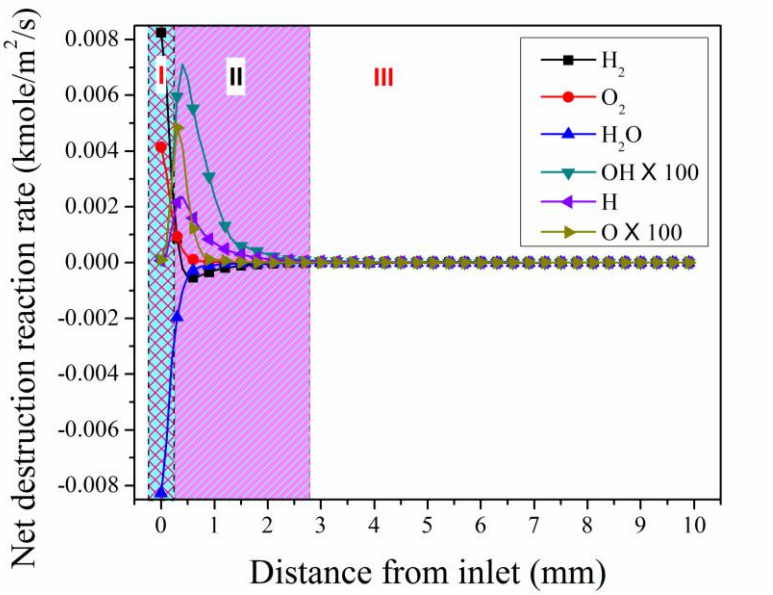

Fig. 7. Net destruction reaction rates of gaseous species on the catalytic surface.

When the gaseous mixture is ignited, the key reactants (H_2 and O_2) concentration sharply

decreases and the mass of free bonds are created in the channel. Thus, the free radical absorption reactions are initiated in the region II. It can be seen in the region II that the net destruction reaction rate of hydrogen atom is greatly higher than that of H_2, and the net destruction reaction rate of H_2 is negative. These results indicate that the fuel desorption reaction (2H(s) => H_2+ 2Pt(s)) rate is higher than that of the fuel absorption reaction (H_2+ 2Pt(s) => 2H(s)) due to the existence of hydrogen atom absorption reaction (H + Pt(s) => H(s)). The free radicals from the homogeneous reaction are drained near the surface, resulting in the interruption of homogeneous reaction. The combustion reaction attains a steady state and the level of the net destruction reaction rate of gaseous species is less than the orders of magnitude of -5 in the region III. The massive product (H_2O) is spread downstream at the region III, and the maximum value of H_2O concentration in the channel is distributed in the downstream. In this case, H_2O can be absorbed and desorbed at the zone, but the net destruction reaction rate of H_2O is also lower.

3.3. Reaction characteristics of key species

The H_2 fuel is rapidly consumed near the inlet in the combustor in region I, and the net destruction reaction rates of H_2 between homogeneous reaction and heterogeneous reaction are used to explain the competition of H_2. The net reaction rates of H_2 for these reactions are shown in Fig. 8 (a). From the variation of reaction rate along the centerline of the channel, it can be noted that the maximum rate of H_2 in HH is lower than that in HR. The decreased reactants are used for participating in the homogeneous reaction in HH when compared with that in HR, showing an inhibition action of heterogeneous reaction on homogeneous reaction. Moreover, the peak rate of destruction of H_2 exists at a wide gap near the inner wall between HH and HR.

During the reaction process, the main destruction reactions of H_2 in homogeneous reaction are

expressed below, R1: H_2+OH = H_2O+H and R2: H_2+O = OH+O. Fig. 8 (b) depicts the reaction rates of R1 and R2 at the vicinity of inner wall (z = 0.485 mm). The reaction rates in HH are much lower than that in HR; it means that the existence of heterogeneous reaction inhibits R1 and R2, due to a high absorption ability of Pt catalyst. The destruction rate of H_2 for the heterogeneous reaction shows a weak intensity near the inlet, because the H_2 sticking coefficient is low (0.046) on the catalytic surface.

The homogeneous reaction is not initiated at inlet, and the fuel diffuse to the surface resulting in a high absorption reaction rate, as seen in Fig. 8 (c). The difference between the destruction rate and creation rate of H_2 near the inlet is much larger than that in the downstream. The small difference between the absorption and desorption reaction rates is displayed, indicating that the reaction rates reach a balance on the downstream surface. Therefore, the fuel depletion is dominant near the inlet, which is in accordance with the analysis in Fig. 7.

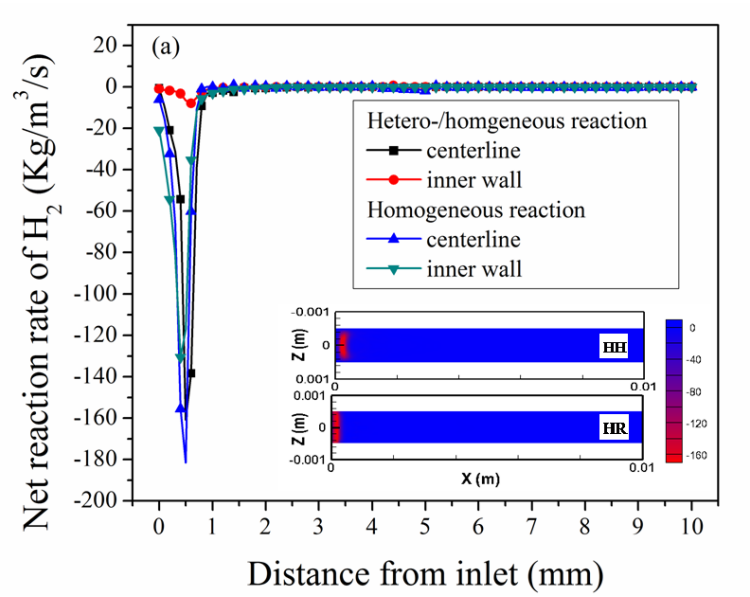

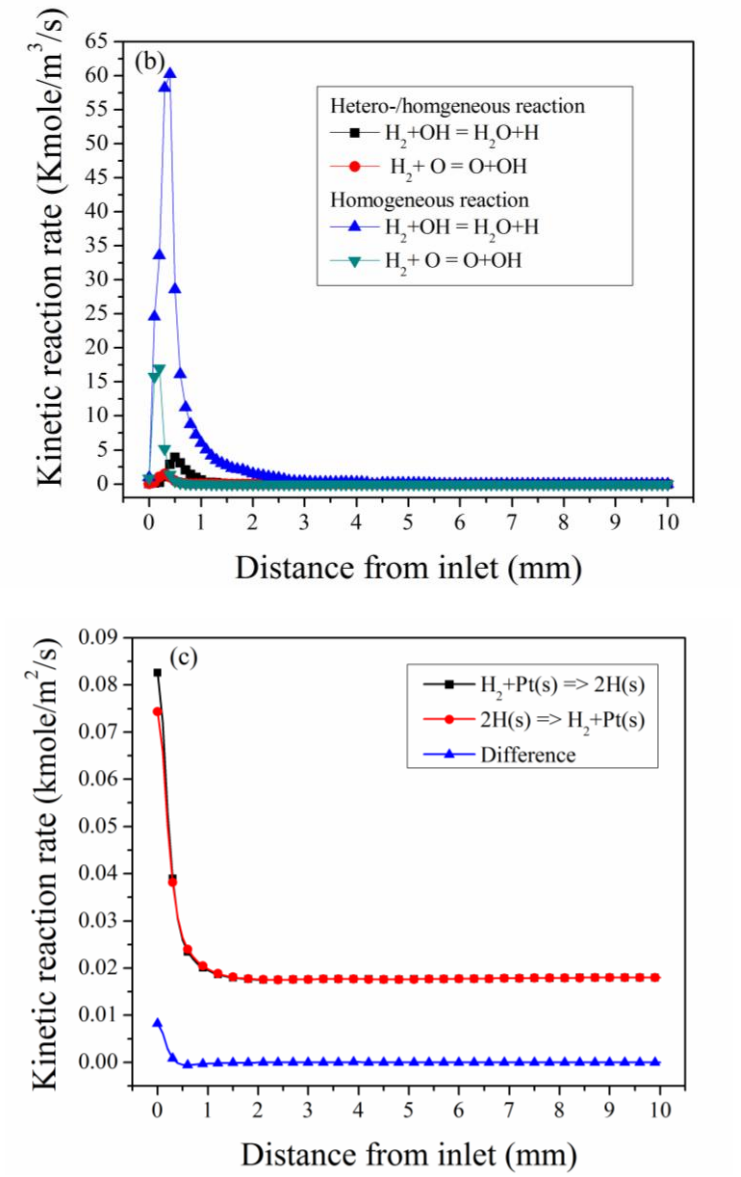

Fig. 8. Destruction rates of H_2 for reactions in HH and HR: (a) net reaction rates of H_2, (b) kinetic reaction rates of R1 and R2, and (c) absorption and desorption reaction rates of H_2 in HH.

When the homogeneous reaction is initiated, the gas-phase chain branching reactions are dominant in the channel. The catalyst possesses high absorption ability for free radicals in the heterogeneous reaction, for example, the stick coefficients of H, O and OH are all 1.0. The free radicals can exactly represent many important reaction characteristics, thus the net reaction rates and creation/destruction rates of OH radical are shown in Fig. 9. The net reaction rate of OH species from Fig. 9 (a) has a positive peak along the centerline of the channel, showing that OH species is created in the channel. In

contrast, a negative peak near the inner wall is observed, which means that the OH species is consumed at this zone. The peak value of the net reaction rate in HH is significantly lower than that of HR, especially for the value near the inner wall, owing to the interruption of chain-branching reaction by absorbed OH species. Fig. 9 (b) shows the absorption/desorption reaction rates of OH radical. The reaction rate is multiplied by a given factor for the comparison, and the reaction rates between the absorption and desorption reactions differ by two orders of magnitude. The absorption rate of OH radical is higher than the desorption rate. In other words, a mass of OH radical from homogeneous reaction can be absorbed near the surface. In this case, the homogeneous reaction (e.g. R1) involving the OH radical should be intercepted near the catalytic surface, which is further interpreted by the decreased reaction rate of R1 in HH. In addition, the absorbed H and O species are not desorbed on the catalytic surface. It should be noted in Fig. 7 that the net desorption reaction rates of free radicals are remarkably higher than that of the fuel. Moreover, the desorption reaction rates of the fuel and product are higher than their absorption reaction rates. It is concluded that the free radicals from homogeneous reaction are absorbed on the catalytic surface, resulting in an inhibiting effect on the propagation reactions.

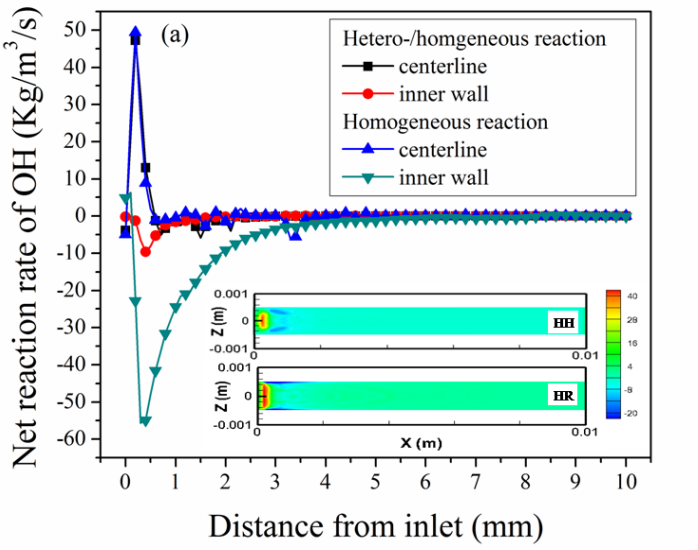

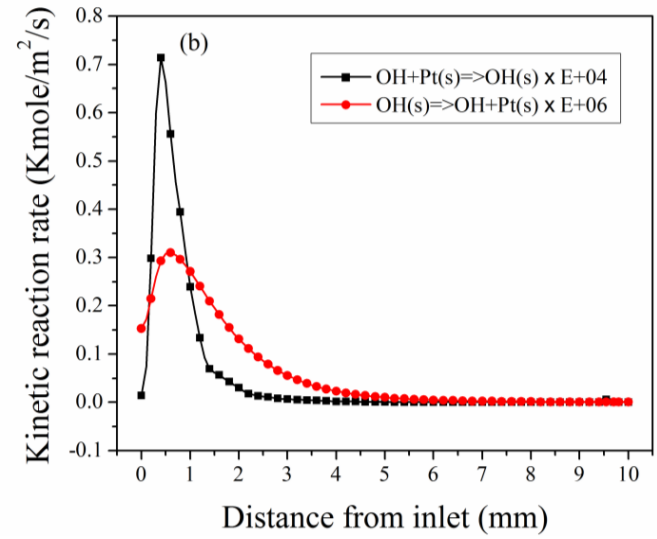

Fig. 9. (a) Net reaction rates of OH radical in HH and HR and (b) kinetic reaction rates of creation/destruction of OH radical on the catalytic surface.

Fig. 10 (a) displays the distribution of H_2O concentration on the centerline of the channel and the inner wall. The mass fraction of H_2O in the downstream is higher than that near the inlet, suggesting that the created H_2O in HH is higher than that in HR from the inserted image in Fig. 10 (a). The increased product indicates that the presence of heterogeneous reaction can improve H_2 conversion rate. The absorption/desorption rates of H_2O along the centerline of the catalytic surface are displayed in Fig. 10 (b). The absorption reaction rate of H_2O on the catalytic surface keeps the linear increasing trend, so is the H_2O desorption reaction rate. Furthermore, the difference between desorption and absorption rate in Fig. 10(b) indicates the relatively high rates near the inlet, suggesting that the catalytic product of H_2O is created here. When the desorbed H_2O diffuses to flow zone, it serves as a third body to promote the chain terminating reaction generally. The elementary reaction is as follows: $H + O_2 + M = HO_2 + M$, where the M is the third body. The high third-body efficiency is enhanced with increasing the concentration of desorbed H_2O, which assists the efficiency in three-body reactions to retard the homogeneous reaction. Moreover, the desorbed H_2O can take away the heat of formation of

homogeneous reaction, leading to a decrease in the gaseous temperature at the reaction zone, which was confirmed in our previous study [29].

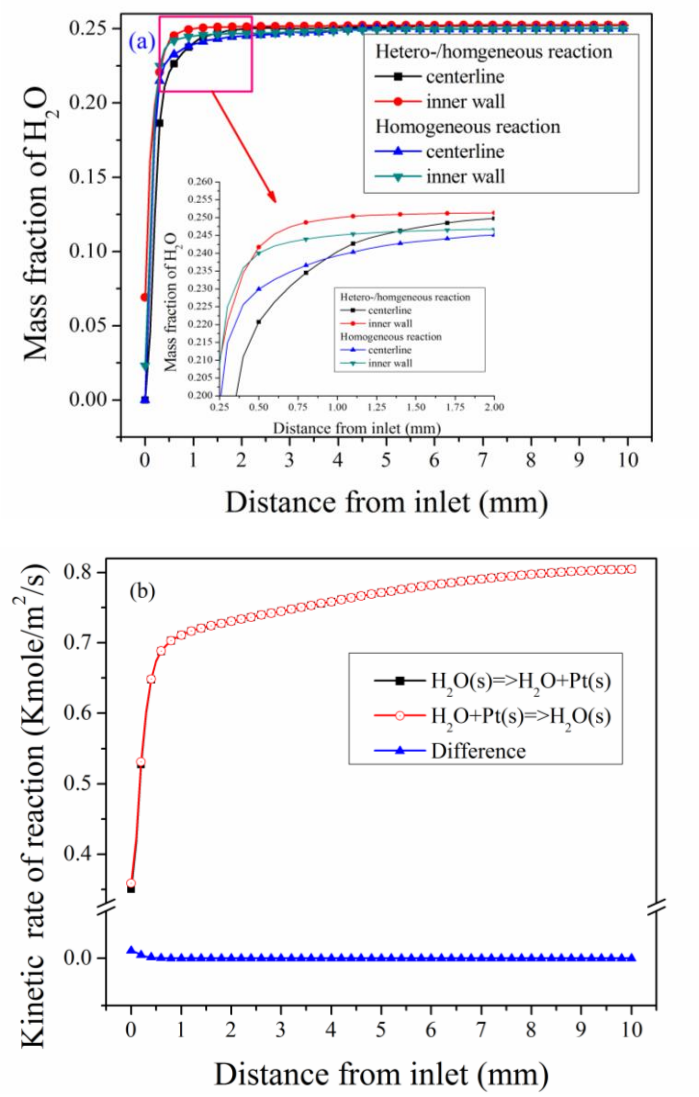

Fig. 10. (a) H_2O concentration profiles on the centerline of the channel and inner wall, and (b) the profiles of absorption/desorption rates of H_2O on the catalytic surface.

3.4. Competitiveness of heterogeneous reaction

The competitiveness of heterogeneous reaction in HH is used to clarify the influence of the heterogeneous reaction on the homogeneous reaction. The competitiveness of heterogeneous reaction reflects the reaction intensity in the combustor, denoted by the Eq. (2) as follows:

$$K_i = \frac{A_i}{B_i} \quad (2)$$

Where A_i is the destruction (or creation) rate of the species i in the heterogeneous reaction, B_i is the total destruction rate of the species i in the whole combustor, K_i is the competitiveness value of heterogeneous reaction of the species i.

Fuel is consumed by homogeneous reaction and heterogeneous reaction in HH, and the K value of fuel is 14.85%. The K value of the product is 28.8%, suggesting that the amount of created H_2O in homogeneous reactions accounts for 71.2% of total product. The K value of product rises as compared with that of fuel because a great deal of gaseous species, such as free radicals and reactants, is absorbed to initiate the heterogeneous reaction for increasing in productivity of H_2O. Furthermore, the homogeneous reaction can create mass intermediate product, resulting in a decrease in yield of H_2O. Meanwhile, the by-product does not exist in the heterogeneous reaction process. The larger K value exists in HH, the stronger competitiveness of heterogeneous reaction is displayed. When the K value is large, the intense inhibition effect of the heterogeneous reaction can terminate the homogeneous reaction. It should be noted that the homogeneous reaction is dominant in catalytic combustor.

4. Conclusions

The heterogeneous and homogeneous reaction characteristics were investigated in the catalytic micro combustor via numerical simulation. A numerical model was established with detailed homogeneous and heterogeneous reaction mechanisms of premixed H_2/air mixture in the micro combustor. The simulation results were verified by experimental data. It has been shown that, the decrease of flame temperature and OH concentration in the channel represents an inhibition influence of heterogeneous reaction on homogeneous reaction. Meanwhile, the heterogeneous reaction process on the catalytic surface is divided into three stages; the rapid depletion of reactants, fast consumption of

free radicals and reaction balance state. The incoming reactants are significantly consumed to initiate heterogeneous reaction near the inlet. The absorbed free radicals interdict the homogeneous reaction at the vicinity of catalytic surface, resulting in the occurrence of the suppression effect of heterogeneous reaction. The final product (H_2O) can enhance the third-body effect to terminate homogeneous reaction. Therefore, the homogeneous reaction plays a dominant role in the catalytic combustion process, and the existence of heterogeneous reaction can reduce the yield of by-product and improve the fuel conversion rate.

Acknowledgements

The authors wish to acknowledge the research grant from National Science Foundation of China (No. 51376082 and 51676088), Natural Science grant of Jiangsu province (No. BK20131253), the Project Funded by the Priority Academic Program Development of Jiangsu Higher Education Institutions (PAPD) and the postgraduate scientific research and innovation projects of Jiangsu Province (KYLX16_0891).

References

[1] Chou S K, Yang W M, Chua K J, Li J, Zhang K L. Development of micro power generators–A review. Applied Energy, 2011, 88(1):1–16.

[2] Ju Y, Maruta K. Microscale combustion: Technology development and fundamental research. Progress in Energy and Combustion Science, 2011, 37(6):669–715.

[3] Yang W M, Jiang D Y, Chou S K, Chua K J, Karthikeyan K, H An. Experimental study on micro modular combustor for micro-thermophotovoltaic system application. International Journal of Hydrogen Energy, 2012, 37(12): 9576–9583.

[4] Sari A, Zohrabian A. Simulation study of the effect of feed moisture on autothermal reforming in

short contact time catalytic micro channels. International Journal of Hydrogen Energy, 2014, 39(39):3269–3285.

[5] Cottrell C A, Grasman S E, Thomas M, Martin K B, Sheffield J W. Strategies for stationary and portable fuel cell markets. International Journal of Hydrogen Energy, 2011, 36(13), 7969-7975.

[6] Pianko-Oprych P, Zinko T, Jaworski Z. Simulation of thermal stresses for new designs of microtubular Solid Oxide Fuel Cell stack. International Journal of Hydrogen Energy, 2015, 40:14584–14595.

[7] Arpino F, Massarotti N, Mauro A, Vanoli L. Metrological analysis of the measurement system for a micro-cogenerative SOFC module. International Journal of Hydrogen Energy, 2011, 36(16):10228-10234.

[8] Weinberg F J, Rowe D M, Min G, Ronney P D. On thermoelectric power conversion from heat recirculating combustion systems. Proceedings of the Combustion Institute, 2002, 29(1):941–947.

[9] Pan J F, Yang W M, Tang A K, Chou S K, Duan L, Li X C, et al. Micro combustion in sub-millimeter channels for novel modular thermophotovoltaic power generators. Journal of Micromechanics and Microengineering, 2010, 20(12):125021–125028.

[10] Deutschmann O, Maier L I, Riedel U, Stroemman A H, Dibble R W. Hydrogen assisted catalytic combustion of methane on platinum. Catalysis Today, 59(1):141–150.

[11] Yan Y F, Pan W L, Zhang L, Tang W M, Yang Z Q, Tang Q, et al. Numerical study on combustion characteristics of hydrogen addition into methane–air mixture. International Journal of Hydrogen Energy, 2013, 38(30):13463–13470.

[12] Garcia-Agreda A, Sarli V D, Benedetto A D. Bifurcation analysis of the effect of hydrogen addition on the dynamic behavior of lean premixed pre-vaporized ethanol combustion.

International Journal of Hydrogen Energy, 2012, 37(37):6922–6932.

[13] Yan Y F, Tang W M, Zhang L, Pan W L, Li L Y. Thermal and chemical effects of hydrogen addition on catalytic micro-combustion of methane–air. International Journal of Hydrogen Energy, 2014, 39(33): 19204–19211.

[14] Zhang Y S, Zhou J H, Yang W J, Liu M S, Cen K F. Effects of hydrogen addition on methane catalytic combustion in a micro tube. International Journal of Hydrogen Energy, 2007, 32(9): 1286–1293.

[15] Schultze M, Mantzaras J. Hetero-/homogeneous combustion of hydrogen/air mixtures over platinum: Fuel-lean versus fuel-rich combustion modes. International Journal of Hydrogen Energy, 2013, 38(25): 10654–10670.

[16] Choi W, Kwon S, Shin H D. Combustion characteristics of hydrogen–air premixed gas in a sub-millimeter scale catalytic combustor. International Journal of Hydrogen Energy, 2008, 33(9):2400–2408.

[17] Fanaee S A, Esfahani J A. Two-dimensional analytical model of flame characteristic in catalytic micro-combustors for a hydrogen–air mixture. International Journal of Hydrogen Energy, 2014, 39(9):4600–4610.

[18] Pizza G, Mantzaras J, Frouzakis C E, Tomboulides A G, Boulouchos K. Suppression of combustion instabilities of premixed hydrogen/air flames in microchannels using heterogeneous reactions. Proceedings of the Combustion Institute, 2009, 32(2):3051–3058.

[19] Pizza G, Mantzaras J, Frouzakis C E. Flame dynamics in catalytic and non-catalytic mesoscale microreactors. Catalysis Today, 2010, 155:123–130.

[20] Mantzaras J, Appel C. Effects of finite rate heterogeneous kinetics on homogeneous ignition in

catalytically stabilized channel flow combustion. Combustion and flame, 2002, 130(4): 336–351.

[21] Wang Y, Zhou Z J, Yang W J, Zhou J H, Liu J Z, Wang Z H, et al. Combustion of hydrogen-air in micro combustors with catalytic Pt layer. Energy Conversion and Management, 2010, 51(6):1127–1133.

[22] Vlachos D G. Homogeneous-heterogeneous oxidation reactions over platinum and inert surfaces. Chemical Engineering Science, 1996, 51(10):2429–2438.

[23] Bui P A, Vlachos D G, Westmoreland P R. Homogeneous ignition of hydrogen-air mixtures over platinum. Symposium (International) on Combustion. 1996, 26(1): 1763–1770.

[24] Deutschmann O. Modeling of the Interactions Between Catalytic Surfaces and Gas-Phase. Catalysis Letters, 2015, 145(1):272–289.

[25] Haruta M, Souma Y, Sano H. Catalytic combustion of hydrogen—II. An experimental investigation of fundamental conditions for burner design. International Journal of Hydrogen Energy, 1982, 7(9):729–736.

[26] Appel C, Mantzaras J, Schaeren R, Bombach R, Inauen A, Kaeppeli B, et al. An experimental and numerical investigation of homogeneous ignition in catalytically stabilized combustion of hydrogen/air mixtures over platinum. Combustion and Flame, 2002, 128(1):340–368.

[27] Chen G B, Chen C P, Wu C Y, Chao Y C. Effects of catalytic walls on hydrogen/air combustion inside a micro-tube. Applied Catalysis A: General, 2007, 332(1):89–97.

[28] Ghermay Y, Mantzaras J, Bombach R, Boulouchos K. Homogeneous combustion of fuel-lean $H_2/O_2/N_2$ mixtures over platinum at elevated pressures and preheats. Combustion and Flame, 2011, 158(8): 1491–1506.

[29] Lu Q B, Pan J F, Yang W M, Pan Z H, Tang A K, Zhang Y. Effects of products from

heterogeneous reactions on homogeneous combustion for H_2/O_2 mixture in the micro combustor. Applied Thermal Engineering, 2016, 102: 897–903.

[30] Lu Q B, Pan, J F, Hu S, Tang A K, Shao X. Hetero-/homogeneous combustion of premixed hydrogen–oxygen mixture in a micro-reactor with catalyst segmentation. International Journal of Hydrogen Energy, 2016, 41(28):12387–12396.

[31] Fluent Inc. FLUENT User′s Guide. Lebanon, USA: Fluent Inc, 1999.

[32] Li J, Zhao Z W, Kazakov A, Dryer F L. An updated comprehensive kinetic model of hydrogen combustion. International journal of chemical kinetics, 2004, 36(10): 566–575.

[33] Deutschmann O, Schmidt R, Behrendt F, Warnatz J. Numerical modeling of catalytic ignition. Twenty-Sixth Symposium (International) on Combustion, 1996: 1747–1754.

[34] Kee R J, Dixon-Lewis G, Warnatz J, Coltrin M E, Miller J A. A Fortran Computer Code Package for the Evaluation of Gas-Phase Multicomponent Transport Properties, Report No. SAND86-8246, Sandia National Laboratories, 1996.

[35] Kee R J, Rupley F M, Miller J A. Chemkin II: A Fortran Chemical Kinetics Package for the Analysis of Gas-Phase Chemical Kinetics, Report No. SAND89-8009B, Sandia National Laboratories, 1996.

[36] Coltrin M E, Kee R J, Rupley F M. Surface Chemkin: A Fortran Package for Analyzing Heterogeneous Chemical Kinetics at the Solid Surface‐Gas Phase Interface, Report No. SAND90-8003C, Sandia National Laboratories, 1996.

[37] Tang A K, Xu Y M, Shan C X, Pan J F, Liu Y X. A comparative study on combustion characteristics of methane, propane and hydrogen fuels in a micro-combustor. International Journal of Hydrogen Energy, 2015, 40(46): 16587–16596.

[38] Chen G B, Chao Y C, Chen C P. Enhancement of hydrogen reaction in a micro-channel by catalyst segmentation. International Journal of Hydrogen Energy, 2008, 33(10):2586–2595.

Figure captions

Fig. 1. Schematic of the combustor model.

Fig. 2. Distribution of the centerline temperature in the combustor with different mesh densities.

Fig. 3. Centerline temperature distributions on the outer surface from experiment and simulation under different conditions.

Fig. 4 Computed contour of temperature distribution in X-Y plane for HH and HR.

Fig. 5. Temperature and OH concentration distribution on the centerline of the channel.

Fig. 6. Major species mass fractions averaged over the Y-Z plane.

Fig. 7. Net destruction reaction rates of gaseous species on the catalytic surface.

Fig. 8. Destruction rates of H_2 for reactions in HH and HR: (a) net reaction rates of H_2, (b) kinetic reaction rates of R1 and R2, and (c) absorption and desorption reaction rates of H_2 in HH.

Fig. 9. (a) Net reaction rates of OH radical in HH and HR and (b) kinetic reaction rates of creation/destruction of OH radical on the catalytic surface.

Fig. 10. (a) H_2O concentration profiles on the centerline of the channel and inner wall, and (b) the profiles of absorption/desorption rates of H_2O on the catalytic surface.

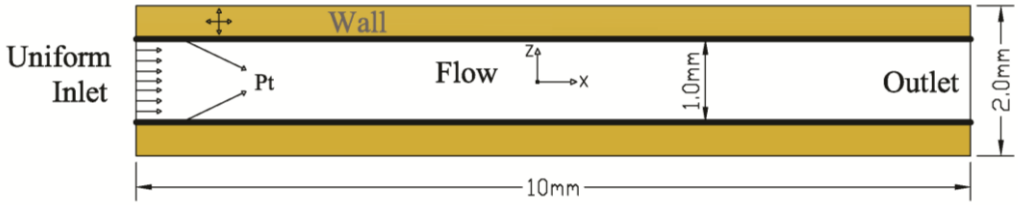

Fig. 1. Schematic of the combustor model.

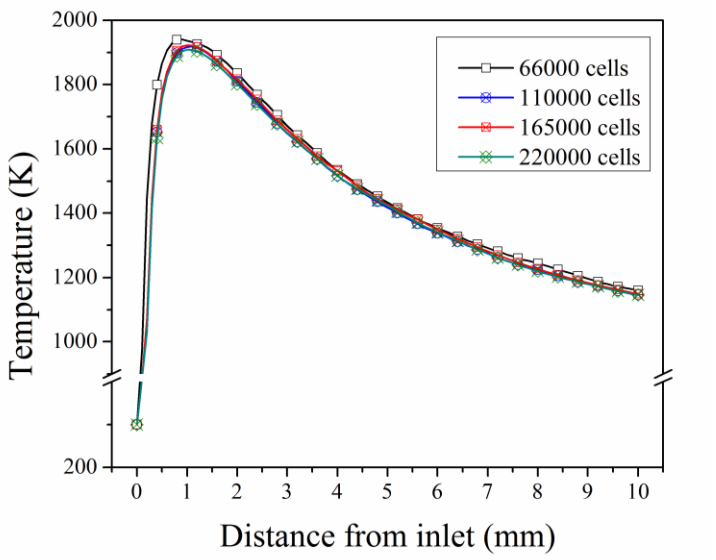

Fig. 2. Distribution of the centerline temperature in the combustor with different mesh densities.

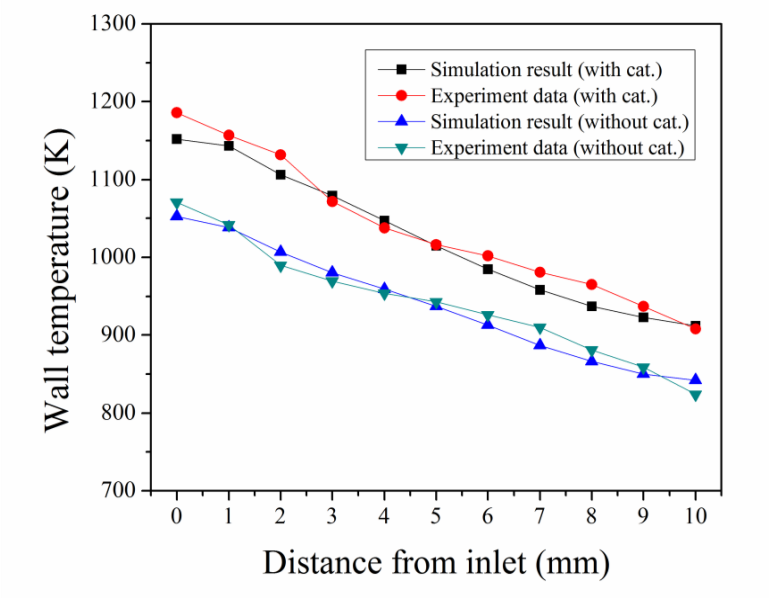

Fig. 3. Centerline temperature distributions on the outer surface from experiment and simulation under different conditions.

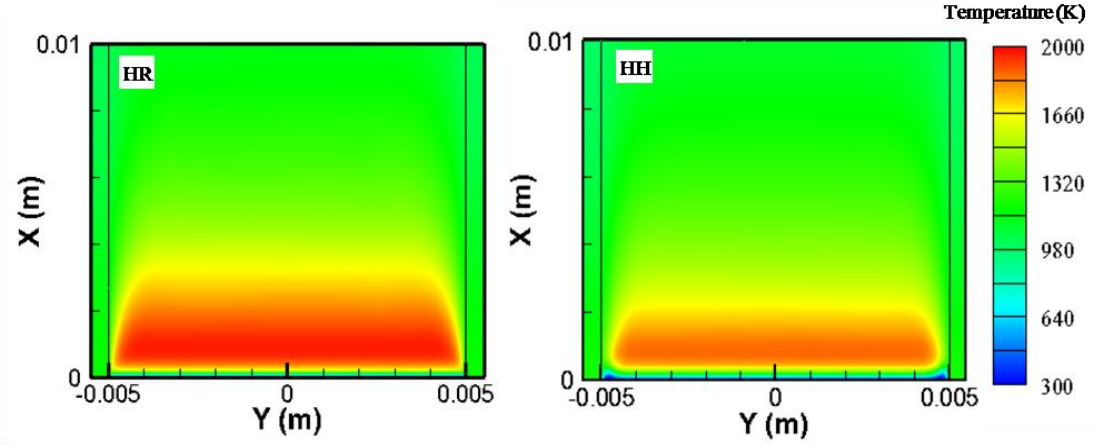

Fig. 4 Computed contour of temperature distribution in X-Y plane for HH and HR.

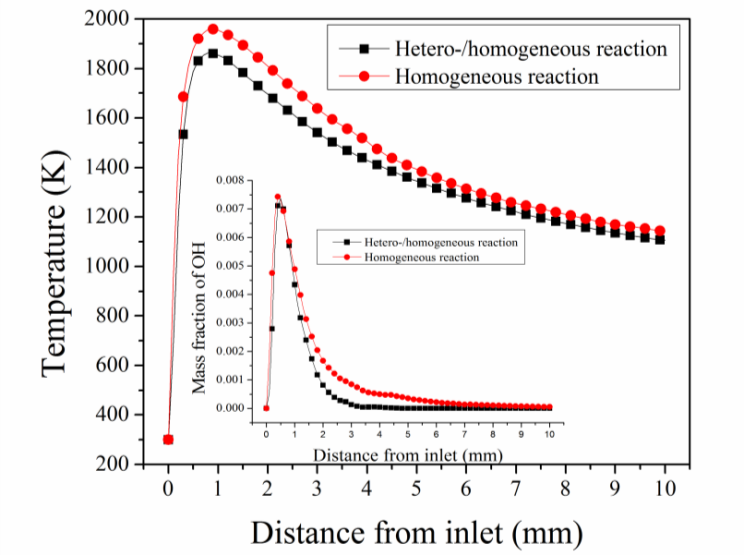

Fig. 5. Temperature and OH concentration distribution on the centerline of the channel.

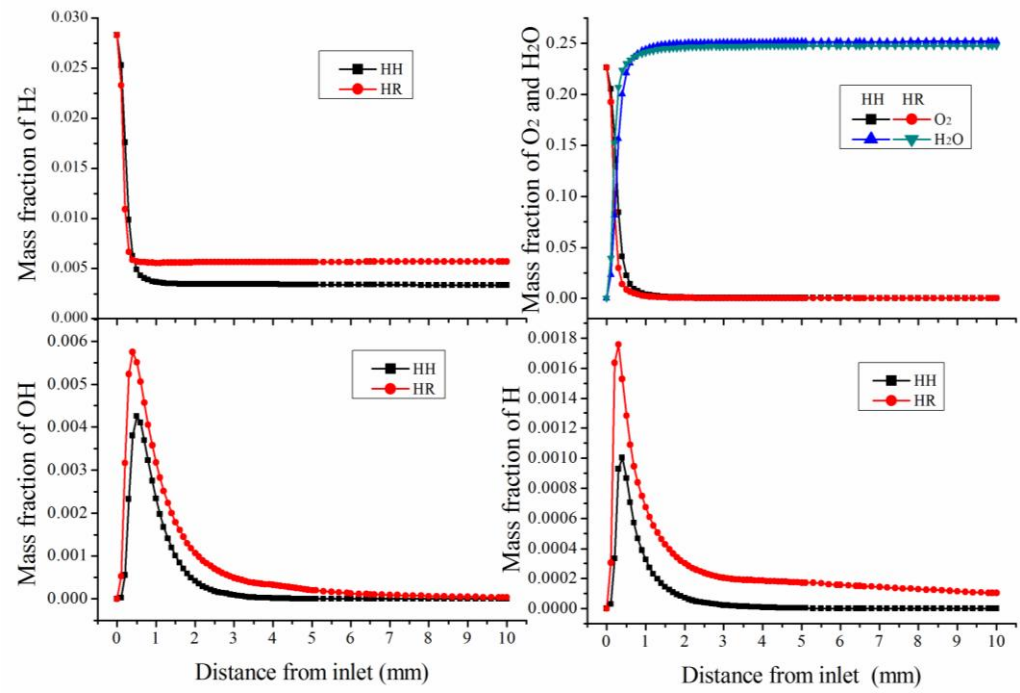

Fig. 6. Major species mass fractions averaged over the Y-Z plane.

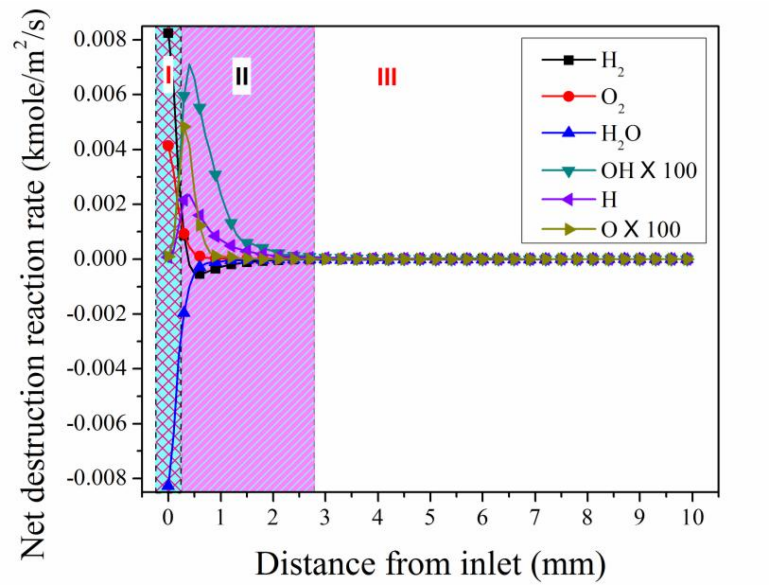

Fig. 7. Net destruction reaction rates of gaseous species on the catalytic surface.

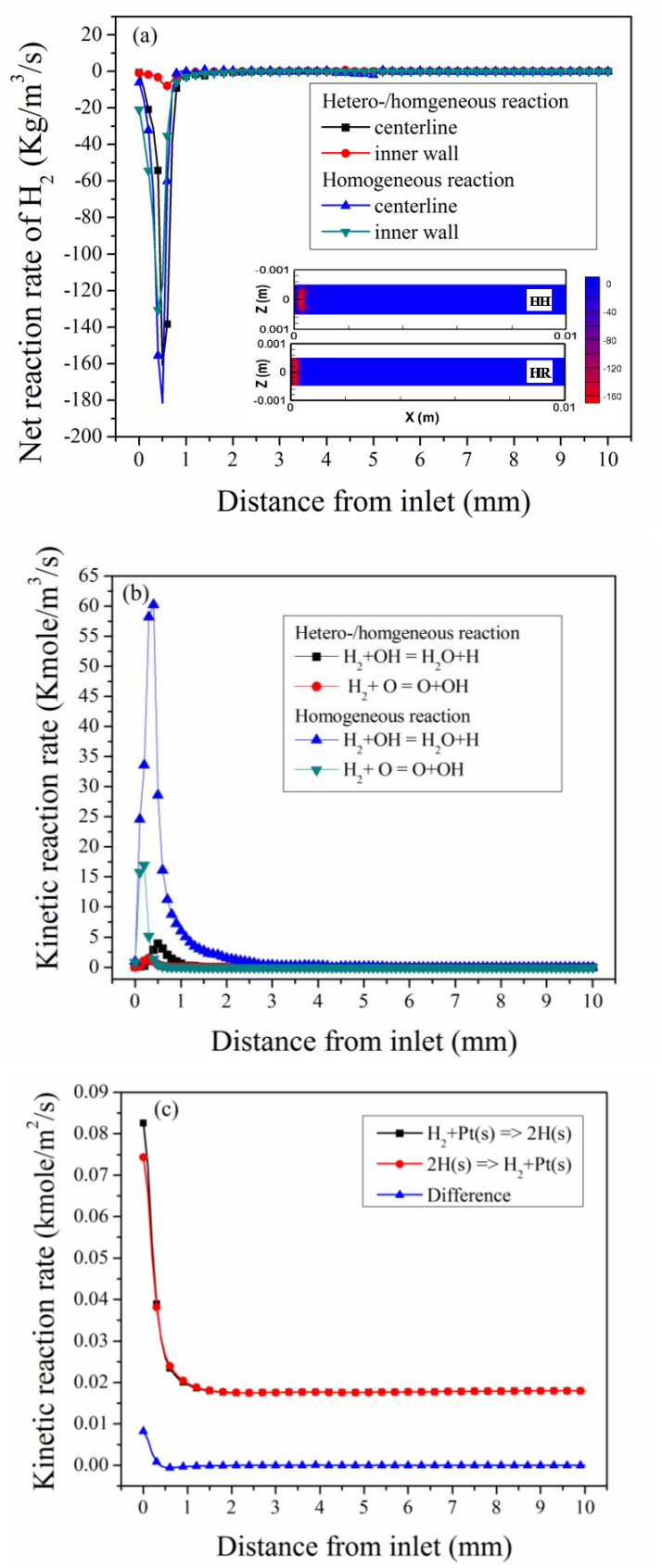

Fig. 8. Destruction rates of H_2 for reactions in HH and HR: net reaction rates of H_2 (a), kinetic reaction rates of R1 and R2 (b), and absorption and desorption reaction rates of H_2 in HH (c).

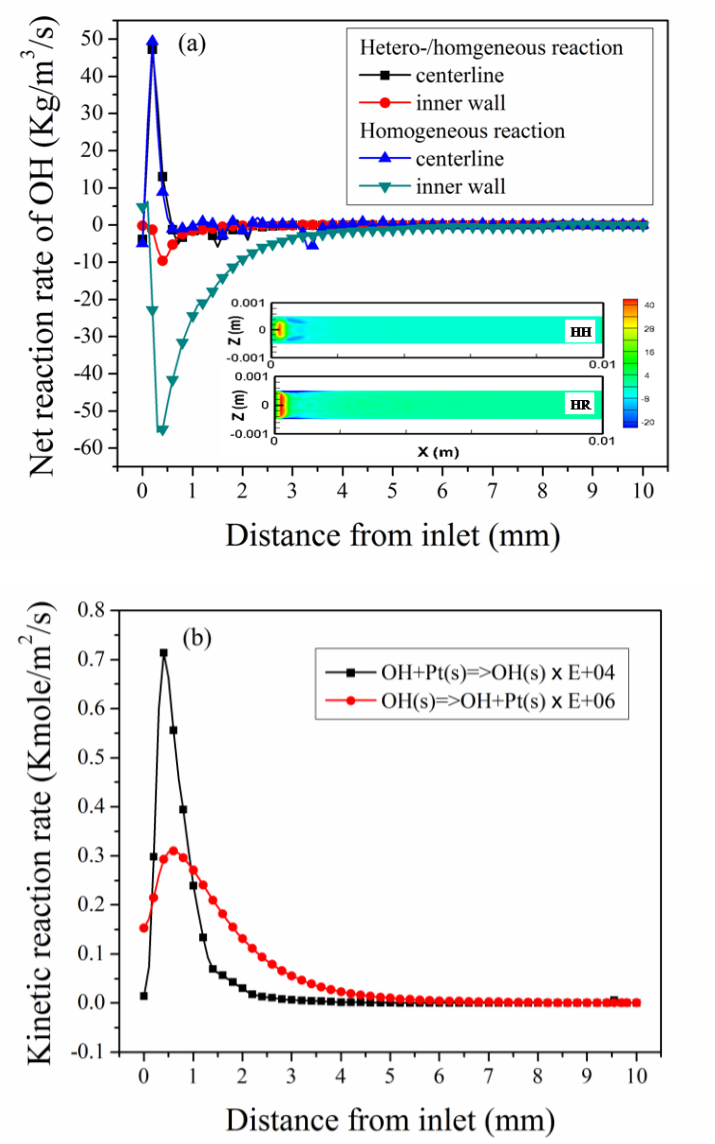

Fig. 9. Net reaction rates of OH radical in HH and HR (a) and kinetic reaction rates of creation/destruction of OH radical on the catalytic surface (b).

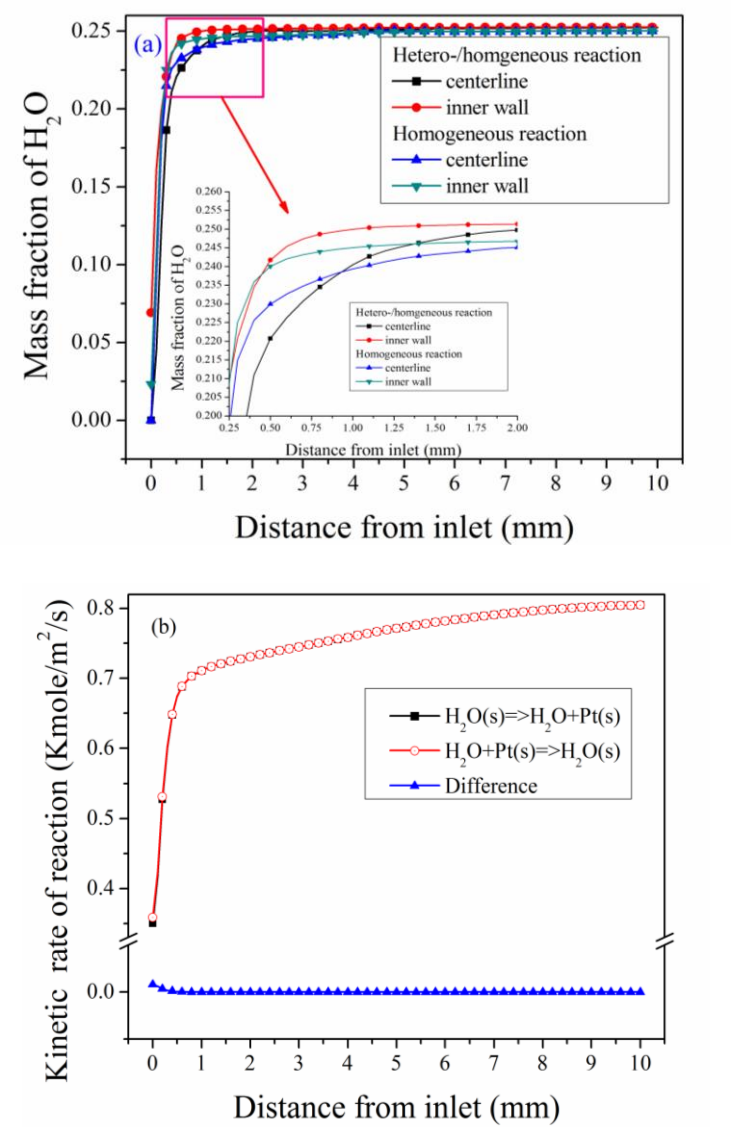

Fig. 10. H_2O concentration profiles on the centerline of the channel and inner wall (a), and the profiles of absorption/ desorption rates of H_2O on catalytic surface (b).